Comprehensive model for studying noise induced by self-homodyne detection of backward Rayleigh scattering in optical fibers

Michael Fleyer,[1,*] James P. Cahill,[2,3] Moshe Horowitz,[1] Curtis R. Menyuk,[2] and Olukayode Okusaga[4]

[1]*Technion - Israel Institute of Technology, Haifa 3200, Israel*
[2]*University of Maryland Baltimore County, Baltimore, Maryland 21250, USA*
[3]*United States Army Research Laboratory, Adelphi, Maryland, 20873, USA*
[4]*The Johns Hopkins University Applied Physics Laboratory, 11100 Johns Hopkins Rd, Laurel, MD 20723, USA*
[*]*mikef@tx.technion.ac.il*

Abstract: Backward Rayleigh scattering in optical fibers due to the fluctuations that are "frozen-in" to the fiber during the manufacturing process may limit the performance of optical sensors and bidirectional coherent optical communication systems. In this manuscript we describe a comprehensive model for studying intensity noise induced by spontaneous Rayleigh backscattering in optical systems that are based on self-homodyne detection. Our model includes amplitude and frequency noise of the laser source, random distribution of the scatterers along the fiber, and phase noise induced in fibers due to thermal and mechanical fluctuations. The model shows that at frequencies above about 10 kHz the noise spectrum is determined by the laser white frequency noise. The laser flicker frequency noise becomes the dominant effect at lower frequencies. The noise amplitude depends on the laser polarization. A very good agreement between theory and experiment is obtained for fibers with a length between 500 m to 100 km and for a laser with a linewidth below 5 kHz.

OCIS codes: (290.1350) Scattering; (290.5870) Rayleigh.

References and links

1. C. K. Kirkendall and A. Dandridge, "Overview of high performance fibre-optic sensing," J. Phys. (Paris) D: Appl. Phys. **37**(18), R197–R216 (2004).
2. M. Froggatt and J. Moore, "High-spatial-resolution distributed strain measurement in optical fiber with Rayleigh scatter," Appl. Opt. **37**(10), 5162–5164 (1998).
3. E. Ip, A. P. T. Lau, D. J. F. Barros, and J. M. Kahn, "Coherent detection in optical fiber systems," Opt. Express **16**(2), 753–791 (2008).
4. R. K. Staubli and P. Gysel, "Crosstalk penalties due to coherent Rayleigh noise in bidirectional optical communication systems," J. Lightwave Technol. **9**(3), 375–380 (1991).
5. U. H. Hong, K. Y. Cho, Y. Takushima, and Y. C. Chung, "Effects of Rayleigh backscattering in long-reach RSOA-based WDM PON," in *Optical Fiber Communication Conference*, 2010 OSA NFOEC (Optical Society of America, 2010), paper OThG1.
6. P. Gysel and R. K. Staubli, "Statistical properties of Rayleigh backscattering in single-mode fibers," J. Lightwave Technol. **8**(4), 561–567 (1990).

#242975 Received 22 Jun 2015; revised 3 Sep 2015; accepted 4 Sep 2015; published 22 Sep 2015

7. O. Okusaga, W. Zhou, J. Cahill, A. Docherty, C. R. Menyuk, "Optical scattering induced noise in RF-photonic systems," in *Proceedings of IEEE Conference on Frequency Control* (IEEE, 2011) pp. 1–6.
8. O. Okusaga, W. Zhou, J. Cahill, A. Docherty, C. R. Menyuk, "Fiber-induced degradation in RF-over-fiber links," *Proceedings of IEEE Conference on Frequency Control* (IEEE, 2012) pp. 1–5.
9. J. P. Cahill, O. Okusaga, W. Zhou, C. R. Menyuk, and G. M. Carter, "Superlinear growth of Rayleigh scattering-induced intensity noise in single-mode fibers," Opt. Express **23**(5), 6400–6407 (2015).
10. S. A. Diddams, "The evolving optical frequency comb [Invited]," J. Opt. Soc. Am. B **27**(11), B51–B62 (2010).
11. N. L. Laberge, V. V. Vasilescu, C. J. Montrose, and P. B. Macedo, "Equilibrium compressibilities and density fluctuations in $K_2O - SiO_2$ glasses," J. of the American Ceramic Society **56**(10), 506–509 (1973).
12. J. Schroeder, R. Mohr, P. B. Macedo and C. J. Montrose, "Rayleigh and Brillouin scattering in $K_2O - SiO_2$ glasses," J. American Ceramic Society **56**(10), 510–514 (1973).
13. T. Watanabe, K. Saito, and A. J. Ikushima, "Fictive temperature dependence of density fluctuation in SiO_2 glass," J. Appl. Phys. **94**(8), 4824–4827 (2003).
14. R. Le Parc, B. Champagnon, C. Levelut, V. Martinez, L. David, A. Faivre, I. Flammer, J. L. Hazemann, and J. P. Simon, "Density and concentration fluctuations in $SiO_2 - GeO_2$ optical fiber glass investigated by small angle x-ray scattering," J. Appl. Phys. **103**(9), 094917 (2008).
15. C. Levelut, A. Faivre, R. Le Parc, B. Champagnon, J.-L. Hazemann, and J.-P. Simon, "In situ measurements of density fluctuations and compressibility in silica glasses as a function of temperature and thermal history," Phys. Rev. B **72**(22), 22421 (2005).
16. M. E. Froggatt and D. K. Gifford, "Rayleigh backscattering signatures of optical fibers - their properties and applications," in *Optical Fiber Communication Conference*, OSA Technical Digest (online) (Optical Society of America, 2013), paper OW1K.6.
17. S. T. Kreger, D. K. Gifford, M. E. Froggatt, B. J. Soller, and M. S. Wolfe, "High resolution distributed strain or temperature measurements in single- and multi-mode fiber using swept-wavelength interferometry," in *Optical Fiber Sensors Conference*, OSA Technical Digest (CD) (Optical Society of America, 2006), paper ThE42.
18. K. H. Wanser, "Fundamental phase noise limit in optical fibres due to temperature fluctuations," Electron. Lett. **28**(1), 53–54 (1992).
19. L. Z. Duan,"Intrinsic thermal noise of optical fibres due to mechanical dissipation," Electron. Lett. **46**(22), 1515–1516 (2010).
20. R. E. Bartolo, A. B. Tveten, and A. Dandridge, "Thermal phase noise measurements in optical fiber interferometers," IEEE J. Quantum Electron. **48**(5), 720–727 (2012).
21. J. Minář, H. de Riedmatten, C. Simon, H. Zbinden, and N. Gisin, "Phase-noise measurements in long-fiber interferometers for quantum-repeater applications," Phys. Rev. A **77**(5), 052325 (2008).
22. R. M. Herman and M. A. Gray, "Theoretical prediction of the stimulated thermal Rayleigh scattering in liquids," Phys. Rev. Lett. **19**(15), 824–828 (1967).
23. T. Zhu, X. Bao, L. Chen, H. Liang, and Y. Dong, "Characteristics of stimulated Rayleigh scattering in optical fibers," Proc. SPIE **7753**, 77532R (2011).
24. R. C. Jones, "A new calculus for the treatment of optical systems," J. Opt. Soc. Am. **31**(7), 488–493 (1941).
25. M. O. Van Deventer, "Polarization properties of Rayleigh backscattering in single-mode fibers," J. Lightwave Technol. **11**(12), 1895–1899 (1993).
26. F. Corsi, A. Galtarossa, and L. Palmieri, "Polarization mode dispersion characterization of single-mode optical fiber using backscattering technique," J. Lightw. Technol. **16**(10), 1832–1843 (1998).
27. R. W. Boyd, *Nonlinear Optics*, 3rd ed. (Elsevier, 2008).
28. Y. Yamamoto, "AM and FM quantum noise in semiconductor lasers - part I: theoretical analysis," IEEE J. Quantum Electron. **19**(1), 34–46 (1983).
29. K. Saito and A. J. Ikushima, "Reduction of light-scattering loss in silica glass by the structural relaxation of frozen-in density fluctuations," Appl. Phys. Lett. **70**(26), 3504–3506 (1997).
30. A. E. Alekseev and V. T. Potapov, "Noise power spectral density of a fibre scattered-light interferometer with a semiconductor laser source," Quantum Electron. **43**(10), 968 – 973 (2013).
31. P. Healey, "Statistics of Rayleigh backscatter from a single-mode fiber ," IEEE Trans. Commun. Technol. **35**(2), 210–214 (1987).
32. O. Tosoni, S. B. Aksenov, E. V. Podivilov, and S. A. Babin, "Model of a fibreoptic phase-sensitive reflectometer and its comparison with the experiment," Quantum Electron. **40**(10), 887–892 (2010).
33. A. Docherty, C. R. Menyuk, J. P. Cahill, O. Okusaga, and W. Zhou, "Rayleigh-scattering-induced RIN and amplitude-to-phase conversion as a source of length-dependent phase noise in OEOs," IEEE Photonics J. **5**(2), 5500514 (2013).
34. P. K. A. Wai and C. R. Menyuk, "Polarization mode dispersion, decorrelation, and diffusion in optical fibers with randomly varying birefringence," J. Lightwave Technol. **14**(2), 148–157 (1996).
35. I. Reed, "On a moment theorem for complex Gaussian processes," IRE Trans. Inform. Theory **8**(3), 194–195 (1962).
36. C. D. Poole and D. L. Favin, "Polarization-mode dispersion measurement based on transmission spectra through a polarizer," J. Lightw. Technol. **12**(6), 917–929 (1994).

#242975 Received 22 Jun 2015; revised 3 Sep 2015; accepted 4 Sep 2015; published 22 Sep 2015

37. K. Kikuchi, "Effect of l/f-Type FM Noise on semiconductor-laser linewidth residual in high-power limit," IEEE J. Quantum Electron. **25**(4), 684–688 (1989).
38. G. L. Abbas, V. W. S. Chan, and T. K. Yee, "Local-oscillator excess-noise suppression for homodyne and heterodyne detection," Opt. Lett. **8**(8), 419–421 (1983).
39. L. B. Mercer, "1/f frequency noise effects on self-heterodyne linewidth measurements," J. Lightwave Technol. **9**(4), 485–493 (1991).
40. O. Llopis, P. H. Merrer, H. Brahimi, K. Saleh, and P. Lacroix, "Phase noise measurement of a narrow linewidth CW laser using delay line approaches," Opt. Lett. **36**(14), 2713–2715 (2011).
41. I. S. Gradshteyn and I. M. Ryzhik, *Table of Integrals, Series, and Products*, 7th ed. (Academic, 2007).
42. Corning product information, "Corning single-mode optical fiber," (Corning, 2002), http://www.corning.com.
43. G. D. Domenico, S. Schilt, and P. Thomann, "Simple approach to the relation between laser frequency noise and laser line shape," Appl. Opt. **49**(25), 4801–4807 (2010).
44. Teraxion white paper, "Narrow-linewidth semiconductor lasers: one technique does not fit all," (Teraxion, 2011), http://www.teraxion.com.
45. B. E. A. Saleh, M. C. Teich, *Fundamentals of Photonics*, 2nd ed. (Wiley, 2007).
46. A. Galtarossa, L. Palmieri, M. Schiano, and T. Tambosso, "Measurement of birefringence correlation length in long, single-mode fibers," Opt. Lett. **26**(13), 962–964 (2001).

1. Introduction

Optical fiber sensors and their applications have been intensively studied due to their advantageous attributes such as immunity to electromagnetic interference (EMI), light weight, small size, high sensitivity, and the ability to perform sensing over a very long distance [1]. Many of these sensors are based on self-homodyne detection in which the signal interferes with the output of the optical source in order to detect small phase changes. Distributed fiber sensors that are based on Rayleigh backscattering have also been intensively studied [2].

Self-homodyne detection is also used in optical communication systems [3]. In such systems, the noise that is induced by Rayleigh backscattering may deteriorate the performance of bidirectional coherent communication systems [4, 5] since the backscattering adds significant low-frequency noise. The spectrum of backward Rayleigh scattering that is due to laser white frequency noise was calculated in [6]. For the case of self-homodyne detection, the noise spectrum was calculated in that work assuming that the coherence length of the laser, given by the laser white frequency noise, is significantly shorter than the fiber length. Recently, noise induced by Rayleigh backscattering has been experimentally studied using a self-homodyne detection scheme [7–9]. In these recent works, the laser coherence length can be long compared to the fiber length. Long coherence length sources have important applications to precise time and frequency transfer over optical fibers [10]. Thus, there is a need for a comprehensive model that is not limited to sources with a short coherence length.

In this manuscript, we present a comprehensive model to describe the intensity noise spectrum that is induced by Rayleigh backscattering in optical fiber systems that use self-homodyne detection. In these systems, noise is principally due to beating between the backward Rayleigh scattered wave and the source. The main effects that lead to backscattered propagating waves in optical fibers are Rayleigh and Brillouin scattering. When the incident optical power in the fiber is weaker than a few dBm, the dominant effect is the spontaneous Rayleigh scattering caused by inhomogeneities in the refractive index that are "frozen-in" during the transition of the liquid silica to the glassy state [11–14]. The presence of these small-scale density fluctuations has been validated by small-angle x-ray scattering measurements of the silica glass [15]. The density fluctuations can be used as a unique fiber signature, since the scattering pattern does not change over a long period of years [16], unless some external strain or temperature is applied [17].

Our comprehensive model takes into account various effects that are required to accurately model self-homodyne detection of backward Rayleigh scattering in optical fibers. In particular,

#242975 Received 22 Jun 2015; revised 3 Sep 2015; accepted 4 Sep 2015; published 22 Sep 2015

we include in the model the flicker frequency noise of the laser. This noise source, which was not considered in previous models [4, 6], strongly affects the Rayleigh backscattered wave. We also include laser amplitude noise, phase noise that is due to mechanical dissipation and thermal fluctuations in the optical fibers [18–20], and the effect of random birefringence in fibers.

We show that the laser phase noise is converted into intensity noise due to beating of the Rayleigh backscattered wave with the source. The generated noise spectrum has a complex dependence on the frequency and on the spectrum of the laser source. The laser flicker frequency noise is the dominant effect at low frequencies, $f < c/(2nL)$, where L is a fiber length, c is the speed of light in the vacuum, and n is the fiber refractive index. When the laser coherence length is longer than the fiber length, we find a complex dependence of the noise spectrum on the fiber. When the fiber length is longer than the laser coherence length, the noise spectrum is approximately a Lorentzian-shaped with a flicker noise component at low frequencies. For a laser with a long coherence length, the noise spectrum is multiplied by a factor that depends on the laser polarization and varies between $1/3$ to $2/3$.

The theoretical model was compared to experimental results that were obtained for a laser with a narrow linewidth below 5 kHz. We find good quantitative agreement between theory and experimental data at frequencies above 200 Hz for fiber lengths between 6 to 100 km. For shorter fibers with lengths between 500 m to 6 km, we only obtained good agreement at higher frequencies of more than about 500 Hz.

We also found that the phase noise that is due to mechanical dissipation and thermal fluctuations that is accumulated by waves propagating in the fiber [18–20] does not significantly affect the noise spectrum of the self-homodyne detected Rayleigh backscattering. Such phase noise is important in interferometric sensors where the difference between the two interferometer arms is on the order of centimeters [20], so that the effect of laser phase noise is not significant.

Changes in the fiber that are due to fluctuations in environmental conditions will add a strong low-frequency components to the noise spectrum [21]. This noise can be modeled by adding it to the fundamental noise due to mechanical dissipation and thermal fluctuations in fibers. However, since environmental noise depends on the specific perturbation and fiber geometry [21], we do not include it in our model. We attribute the discrepancy between theory and experiment at low frequencies below 500 Hz to this noise source.

For sufficiently high incident power, stimulated Rayleigh scattering may occur [7, 22, 23]. In our experiments, the Rayleigh backscattered power grew approximately linearly with the input optical power when it was changed between 0 to 15 dBm. We conclude that stimulated scattering was not an important factor in our experiments.

2. Rayleigh backscattering model

In this manuscript, we study the intensity noise spectrum that is induced by Rayleigh backscattering in a self-homodyne detection scheme that is pictured in Fig. 1. This scheme was used in the experiments in [9], as described in section 3. A continuous wave (CW) laser source is split into two waves by a fiber coupler. One of these two waves passes through a variable optical power attenuator and is then injected into an optical fiber that is terminated by an isolator. The backscattered Rayleigh wave propagates through the circulator into a coupler and interferes with part of the forward propagating source wave at the photo-detector input. The electrical signal is then obtained with an electrical spectrum analyzer.

We model the laser wave using a complex electrical field phasor:

$$\mathbf{E}_s(t) = \mathbf{p}_s E_s(t), \tag{1}$$

with

$$E_s(t) = E_0\,[1 + m(t)] \exp\left[j\psi(t) + j\omega_0 t\right], \tag{2}$$

#242975 Received 22 Jun 2015; revised 3 Sep 2015; accepted 4 Sep 2015; published 22 Sep 2015

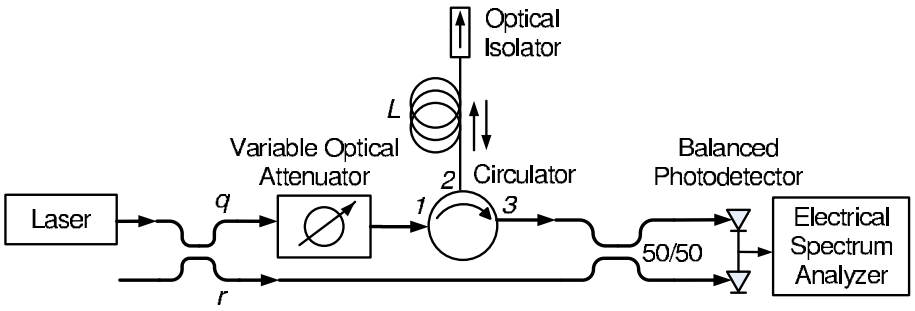

Fig. 1. Schematic description of a system for self-homodyne detection of Rayleigh backscattering induced noise. A continuous wave laser is split by a coupler with power coupling fractions of r and q. One of the two waves (q) passes through a variable optical attenuator that controls the power that is injected into a long optical fiber with a length L. The fiber is terminated by an optical isolator to minimize reflections from the end. The backscattered wave from the optical fiber passes through an optical circulator, interferes with a part of the laser wave (r), and is detected by a pair of balanced photo-detectors. The output signal is measured with an RF spectrum analyzer.

where $m(t)$ is a relative amplitude noise of the source, $\psi(t)$ is a laser phase noise, ω_0 is the carrier frequency, and $\mathbf{p_s}$ is a normalized Jones vector that denotes the laser polarization state [24].

The Rayleigh scattering is modeled by a complex backscattering coefficient $\kappa(z)$ [6] that varies randomly along the fiber length z. The forward propagating wave experiences additive phase noise $\phi(z,t)$ due to mechanical dissipation and thermal fluctuations [18–20], as well as loss that is described by a power loss coefficient per fiber length, α. Additional phase fluctuations are added by environmental perturbations [21]. The mean drift rate of this phase noise varies between 250 rad/s to 1000 rad/s for a 36.5 km fiber [21]. In this manuscript we do not consider this noise in our model, although it may in principle be added to the fiber phase noise $\phi(z,t)$.

The change of the field polarization vector along the fiber can be described for a quasi-monochromatic wave using a Jones matrix $\mathsf{P}(z)$ [6]:

$$\mathbf{p}_s(z) = \mathsf{P}(z)\,\mathsf{T}_1\mathbf{p}_s, \tag{3}$$

where $\mathbf{p}_s$ is the normalized Jones vector of the source, $\mathbf{p}_s(z)$ is the normalized Jones vector as a function of fiber position, T_1 is the Jones matrix that describes the polarization transformation from the laser to the fiber entrance at $z = 0$, and $\mathsf{P}(z)$ is the Jones transformation matrix for the fiber. The polarization state of light that propagates in optical fiber systems that do not use polarization preserving fiber and components will evolve in way that is not known because of birefringence in the fiber and other system components. The Jones matrix T_1 takes this unknown polarization rotation into account.

We define $\mathbf{E}_F(z,t)$ as the forward propagating field at a location z, $\mathbf{E}_R^z$ as the field at the photo-detector input caused by Rayleigh backscattering from a location z, and $\mathbf{E}_R$ as total reflected field at the photo-detector input. The forward propagating laser field phasor at a length z along the fiber is given by

$$\mathbf{E}_F(z,t) = \mathsf{P}(z)\,\mathsf{T}_1\mathbf{p}_s E_s\left(t-\frac{nz}{c}\right)\exp\left[j\int_0^z \mathrm{d}z'\,\frac{\omega_0}{c}\Delta n_e\left(z',t-\frac{n(z-z')}{c}\right)-z\frac{\alpha}{2}\right], \tag{4}$$

where $\Delta n_e(z,t)$ is a refractive index variation due to thermal and thermo-mechanical fluctuations in the optical fiber [18–20] and c is the speed of light in the vacuum.

#242975 Received 22 Jun 2015; revised 3 Sep 2015; accepted 4 Sep 2015; published 22 Sep 2015

Backward Rayleigh scattering in optical fibers is caused due to density fluctuations that are "frozen-in" during the manufacturing process. The field that is backscattered from a location z creates a signal at the photo-detector,

$$\mathbf{E}_R^z(t) = \mathsf{T}_2 \mathsf{P}^T(z)\,\mathbf{E}_F\left(z, t-\frac{nz}{c}\right)\kappa(z)\exp\left[-j\int_z^0 \mathrm{d}z'\,\frac{\omega_0}{c}\Delta n_e\left(z', t-\frac{nz'}{c}\right)-z\frac{\alpha}{2}\right], \quad (5)$$

where $\mathsf{P}^T(z)$ is the transposed Jones matrix that describes the backward propagation of the scattered wave [25, 26], $\kappa(z)$ is the local reflection due to Rayleigh backscattering, and T_2 is the Jones transformation matrix from the entrance to the fiber to the photo-detector.

The total reflected wave at the photo-detector is obtained by integrating the local reflections along the fiber and then substituting Eq. (4) into Eq. (5) to yield

$$\mathbf{E}_R(t) = \int_0^L \mathrm{d}z\;\mathsf{T}_2\mathsf{P}^T(z)\,\mathsf{P}(z)\,\mathsf{T}_1\mathbf{p}_s E_s\left(t-\frac{2nz}{c}\right)\kappa(z)\exp(-\alpha z)\exp[j\phi(z,t)], \quad (6)$$

where $\phi(z,t)$ denotes the total phase fluctuations induced by the fiber during the forward and backward propagation,

$$\phi(z,t) = \int_0^z \mathrm{d}z'\,\frac{\omega_0}{c}\Delta n_e\left(z', t-\frac{n(2z-z')}{c}\right) - \int_z^0 \mathrm{d}z'\,\frac{\omega_0}{c}\Delta n_e\left(z', t-\frac{nz'}{c}\right). \quad (7)$$

We assume that the phase noise $\phi(z,t)$ varies on a time scale that is significantly longer than the round-trip propagation time of the light in the fiber. Hence, the phase noise adds coherently during backward and forward propagation and the two terms in Eq. (7) are approximately the same.

The total electrical field $\mathbf{E}(t)$ at the photo-detector is given by

$$\mathbf{E}(t) = \exp(j\gamma_0)\,r\mathsf{T}_{\mathrm{ref}}\mathbf{E}_s(t) + qlE_R(t), \quad (8)$$

where r and q are the complex coupling coefficients of the coupler that is connected to the laser, so that $|r|^2+|q|^2=1$, l is the fraction of the field that is transmitted by the variable attenuator, and γ_0 is a constant phase offset. The matrix $\mathsf{T}_{\mathrm{ref}}$ is the Jones matrix that describes the polarization transformation from the source to the photo-detector, and we define $\mathbf{p}_{\mathrm{ref}} = \mathsf{T}_{\mathrm{ref}}\mathbf{p}_s$.

A photo-detector converts the optical field into an electrical voltage [27],

$$V_{\mathrm{RF}}(t) = \frac{1}{2}A_{\mathrm{eff}}R\eta\varepsilon_0 nc|\mathbf{E}(t)|^2 \equiv b|\mathbf{E}(t)|^2, \quad (9)$$

where $|\mathbf{E}(t)|$ denotes the amplitude of the field vector, A_{eff} is a fiber effective cross-section area, η is photo-detector conversion efficiency, ε_0 is the vacuum permittivity, and R is a photo-detector resistivity.

To analyze the RF spectrum of $V_{\mathrm{RF}}(t)$, we first calculate the time–averaged autocorrelation function of Eq. (9),

$$r(\tau) = \langle V_{\mathrm{RF}}(t)V_{\mathrm{RF}}^*(t-\tau)\rangle = b^2\langle|\mathbf{E}(t)|^2|\mathbf{E}(t-\tau)|^2\rangle. \quad (10)$$

To calculate Eq. (10), we use several simplifying assumptions:

#242975 Received 22 Jun 2015; revised 3 Sep 2015; accepted 4 Sep 2015; published 22 Sep 2015

1. The laser source is quasi-monochromatic with amplitude and frequency noise. The laser angular-frequency noise $\Delta\psi(t)$ is a zero mean Gaussian random process [28]. We denote its power spectral density $S_{\Delta\psi}(\omega)$, and we note that the laser phase noise at time t may be written $\psi(t) = \int_0^t \mathrm{dT}\Delta\psi(T)$. We also assume that the relative laser amplitude noise $m(t)$, defined in Eq. (2) is a zero mean Gaussian process with a small amplitude $[|m(t)| \ll 1]$, and we write its autocorrelation function as $r_m(\tau) = \langle m(t)m^*(t-\tau)\rangle$.

2. During the light propagation through the fiber, phase noise ϕ is added to the optical signal due to thermal and thermo-mechanical fluctuations in the optical fiber [18–20]. A model of both effects gives a very good agreement with the experimental data at frequencies as low as 30 Hz [20]. The amplitude of the frequency spectrum and hence the auto-correlation function of the phase noise depend linearly on the fiber length L, so that [20]

$$S_\phi(L,\omega) = 4L\left[\alpha_1 F(\omega) + \alpha_2/|\omega|\right]. \tag{11}$$

   The variables α_1 and α_2 and the function $F(\omega)$ depend on the fiber properties, optical wavelength, and the fiber temperature (See e.g. [20]). We assume that the phase noise $\phi(z,t)$ varies on a time scale that is much longer than the round-trip propagation time of the light in the fiber. Hence, the phase noise adds coherently during backward and forward propagation and the auto-correlation function is four times larger than it would be with one way transmission.

   Additional phase noise is added by environmental perturbations [21]. This noise is often significantly higher than the fundamental noise due to thermal and thermo-mechanical fluctuations in fibers, and it may also have a mean drift rate [21]. However, since this noise depends on the specific environmental perturbations and fiber geometry [21], we do not include it in our model. In principle, it can be directly added to the fundamental phase noise induced in fibers, denoted by ϕ in Eq. (7).

3. Rayleigh scattering in fibers is created by material density fluctuations that are "frozen-in" during the transition of the glass from liquid to solid state [11–15, 29]. It has been shown that these fluctuations do not change over a period of years [16], except when slowly varying external effects cause some shift in the scattering spectrum [17]. In a single experiment only one fiber with a specific realization of the Rayleigh scatterers is used. However, slow additive phase noise due to environmental changes and slow frequency noise of the laser source cause temporal fluctuations of the Rayleigh backward wave [30]. Assuming that the measurement duration is sufficiently long, the ensemble average of the Rayleigh scattering coefficients can be replaced by its time average. Hence, we assume that backscattering coefficient per unit of length $\kappa(z)$ are randomly distributed along the fiber and can be modeled by a complex white Gaussian zero mean random process, whose real and imaginary parts are statistically independent [6, 30–32],

$$\langle \kappa(z_1)\kappa^*(z_2)\rangle \approx \sigma_\kappa^2 \delta(z_1 - z_2), \tag{12}$$

   where $\langle\rangle$ denotes time average on the order of a second that is longer than typical time associated with phase changes due to environmental perturbations.

4. We neglect amplitude to phase (AM-PM) and amplitude to amplitude (AM-AM) noise conversion in the photo-detector. Recent measurements of the noise conversion coefficients (see [33], Fig. 6) indicate that for sufficiently low incident optical powers ($P_{in} < 1$ mW) the AM-AM noise gain is very close to unity, and the AM-PM noise gain

#242975 Received 22 Jun 2015; revised 3 Sep 2015; accepted 4 Sep 2015; published 22 Sep 2015

is negligible. The photo-detector shot noise was added to our numerical calculations as an independent noise that depends on the average power.

5. We assume that there is no polarization-dependent loss in the system [34], so that all the Jones matrices, T_1, T_2, T_{ref}, and $\mathsf{P}(z)$ are unitary [26]. It follows in particular that $\mathsf{P}^{\dagger}(z)\mathsf{P}(z) = \mathsf{P}^{-1}(z)\mathsf{P}(z) = \mathsf{I}$, where I is the identity matrix. We also assume a low-birefringent fiber with length that is much longer than both the polarization beat length (L_{B}) and the polarization correlation length (L_{C}) as defined in [34].

6. We assume that the different noise sources (laser amplitude noise, laser phase noise, fiber phase noise, fiber scattering coefficients, and random fiber birefringence) are statistically independent. We also assume that all the time-varying random processes are stationary and ergodic. Hence time-average can be replaced by an ensemble average.

Substitution of Eq. (8) into Eq. (10) yields a sum of 16 terms; however, due to statistical properties of the backscattering coefficient κ, only six of them yield a non-zero results that depend on τ [35],

$$\begin{aligned} r(\tau)/b^2 = &\left\langle |r\mathbf{E}_s(t)|^2 |r\mathbf{E}_s(t-\tau)|^2 \right\rangle + \left\langle |lq\mathbf{E}_R(t)|^2 |lq\mathbf{E}_R(t-\tau)|^2 \right\rangle + \\ &\left\langle |r\mathbf{E}_s(t)|^2 |lq\mathbf{E}_R(t-\tau)|^2 \right\rangle + \left\langle |r\mathbf{E}_s(t-\tau)|^2 |lq\mathbf{E}_R(t)|^2 \right\rangle + \\ &2|r|^2|q|^2 l^2 \,\mathrm{Re}\left\langle \mathbf{E}_R^{\dagger}(t)\,\mathbf{p}_{\text{ref}} E_s(t)\, E_s{}^*(t-\tau)\,\mathbf{p}_{\text{ref}}^{\dagger}\mathbf{E}_R(t-\tau) \right\rangle. \end{aligned} \tag{13}$$

The first term in Eq. (13), $\left\langle |r\mathbf{E}_s(t)|^2 |r\mathbf{E}_s(t-\tau)|^2 \right\rangle$ is due to a direct contribution of the laser intensity noise, so that

$$\left\langle |r\mathbf{E}_s(t)|^2 |r\mathbf{E}_s(t-\tau)|^2 \right\rangle \approx 2|E_0|^4 |r|^4 \left[r_m(\tau) + O\left(r_m^2\right) \right], \tag{14}$$

where the $r_m(\tau)$ is the autocorrelation function of the laser amplitude noise that we previously defined. The second term $\left\langle |lq\mathbf{E}_R(t)|^2 |lq\mathbf{E}_R(t-\tau)|^2 \right\rangle$ is caused by the Rayleigh backscattered intensity noise and it is on the order of σ_κ^4. A detailed statistical analysis of this term is given in [6]. Since the Rayleigh backscattering intensity is low, this term can be neglected with respect to the beating terms analyzed next that are on the order of σ_κ^2. The third and fourth terms are due to beating of the laser and the backscattered intensity noise,

$$\begin{aligned} &\left\langle |r\mathbf{E}_s(t)|^2 |lq\mathbf{E}_R(t-\tau)|^2 \right\rangle + \left\langle |r\mathbf{E}_s(t-\tau)|^2 |lq\mathbf{E}_R(t)|^2 \right\rangle \approx \\ &2|r|^2|q|^2 l^2 |E_0|^4 \sigma_\kappa^2 \int_0^L \mathrm{d}z \,\left[r_m(2nz/c+\tau) + r_m(2nz/c-\tau) + O\left(r_m^2\right) \right]. \end{aligned} \tag{15}$$

The last term in Eq. (13) results from the phase noise in the source signal and the Rayleigh backscattered signal that are converted into intensity noise due to the beating between the two waves,

$$\begin{aligned} &\left\langle \mathbf{E}_R^{\dagger}(t)\,\mathbf{p}_{\text{ref}} E_s(t)\, E_s{}^*(t-\tau)\,\mathbf{p}_{\text{ref}}^{\dagger}\mathbf{E}_R(t-\tau) \right\rangle = \\ &l^2|q|^2|r|^2\sigma_\kappa^2 \int_0^L \mathrm{d}z \exp(-2\alpha z)\, R_{\text{fiber}}(z,\tau) T_P(z) \times \\ &\left\langle E_s(t) E_s^*(t-\tau) E_s^*\left(t-\frac{2nz}{c}\right) E_s\left(t-\frac{2nz}{c}-\tau\right) \right\rangle, \end{aligned} \tag{16}$$

#242975 Received 22 Jun 2015; revised 3 Sep 2015; accepted 4 Sep 2015; published 22 Sep 2015

where

$$R_{\text{fiber}}(z,\tau) = \langle \exp\left[j\phi(z,t-\tau) - j\phi(z,t)\right]\rangle \tag{17}$$

is the auto-correlation function related to the phase noise induced in the fiber, and

$$T_P(z) = \left|\mathbf{p}_{\text{ref}}^{\dagger}\mathsf{T}_2\mathsf{P}^T(z)\,\mathsf{P}(z)\,\mathsf{T}_1\mathbf{p}_s\right|^2 \tag{18}$$

is a random variable that describes the effect of the polarization change of the backward Rayleigh scattering due to the beating with the source wave. Equation (18) can be written using the Stokes unit vector $\mathbf{s}(z)$ of the reflected field from a location z [36],

$$T_P(z) = \frac{1}{2}\left[1 + \mathbf{s}_{\text{ref}}\cdot\mathbf{s}(z)\right], \tag{19}$$

where $\mathbf{s}_{\text{ref}}$ is a Stokes unit vector of the polarization of the source wave at the photo-detector $\mathbf{p}_{\text{ref}}$. The Stokes unit vector of the Rayleigh backscattered wave at the photo-detector is given by $\mathbf{s}(z) = \mathsf{M}_2\mathsf{M}_{\text{rt}}(z)\mathsf{M}_1\mathbf{s}_0$, where $\mathbf{s}_0$ is the Stokes vector that corresponds to the source polarization Jones vector $\mathbf{p}_s$. The matrices M_1, M_2 and $\mathsf{M}_{\text{rt}}(z)$ are 3×3 reduced Mueller matrices that correspond respectively to the Jones matrices T_1, T_2, and the round-trip matrix $\mathsf{P}^T(z)\mathsf{P}(z)$.

Substitution of Eq. (2) into Eq. (16) gives

$$\begin{aligned}&\left\langle E_s(t)E_s^*(t-\tau)E_s^*\left(t-\frac{2nz}{c}\right)E_s\left(t-\frac{2nz}{c}-\tau\right)\right\rangle = \\ &|E_0|^4\left\langle\left[1+m(t)\right]\left[1+m^*(t-\tau)\right]\left[1+m^*\left(t-\frac{2nz}{c}\right)\right]\left[1+m\left(t-\frac{2nz}{c}-\tau\right)\right]\right\rangle \times \\ &R_{S_{\Delta\psi(\omega)}}(z,\tau),\end{aligned} \tag{20}$$

where

$$R_{S_{\Delta\psi(\omega)}}(z,\tau) = \left\langle \exp\left\{ j\left[\psi(t) - \psi(t-\tau) - \psi\left(t-\frac{2nz}{c}\right) + \psi\left(t-\frac{2nz}{c}-\tau\right)\right]\right\}\right\rangle, \tag{21}$$

is the autocorrelation function of the laser phase noise. We now use the definition of the power spectral density of the angular-frequency noise

$$S_{\Delta\psi}(\omega) = \int_{-\infty}^{\infty} \mathrm{d}\tau\,\langle\Delta\psi(t)\Delta\psi(t+\tau)\rangle\exp\left(-j\omega\tau\right), \tag{22}$$

where $\Delta\psi(t) = \mathrm{d}\psi(t)/\mathrm{d}t$. We also use our assumption that $\Delta\psi(t)$ is a zero-mean, ergodic Gaussian-distributed random process and recall the general relation $\langle\exp\left[jx(t)\right]\rangle = \exp\left[-(1/2)\left\langle x^2(t)\right\rangle\right]$, where $x(t)$ is any zero-mean, Gaussian-distributed real random process [35]. We then find [37]

$$R_{S_{\Delta\psi}(\omega)}(z,\tau) = \exp\left[-\frac{4}{\pi}\int_{-\infty}^{\infty}\mathrm{d}\omega\sin^2\left(\frac{\omega\tau}{2}\right)\sin^2\left(\frac{\omega\tau_z}{2}\right)\frac{S_{\Delta\psi}(\omega)}{\omega^2}\right], \tag{23}$$

where

$$\tau_z = \frac{2nz}{c}$$

is the propagation delay from the reflection at z.

#242975 Received 22 Jun 2015; revised 3 Sep 2015; accepted 4 Sep 2015; published 22 Sep 2015

Since the laser intensity noise $m(t)$ is a zero mean Gaussian process with a small amplitude $[|m(t)| \ll 1]$, Eq. (20) can be approximated using the properties of a Gaussian moments [35],

$$\begin{aligned}&\left\langle E_s(t)E_s^*(t-\tau)E_s^*\left(t-\frac{2nz}{c}\right)E_s\left(t-\frac{2nz}{c}-\tau\right)\right\rangle \approx \\ &|E_0|^4\left[1+2r_m(\tau)+2r_m(\tau_z)+O\left(r_m^2\right)\right]R_{S_{\Delta\psi}(\omega)}(z,\tau).\end{aligned} \tag{24}$$

Using the relation between the optical power and field $P_0 = 1/2A_{\text{eff}}c\varepsilon_0 n|E_0|^2$ and substituting Eqs. (14), (15), (16) and (24) into Eq. (13), the autocorrelation function of the detected electrical signal becomes

$$\begin{aligned}&r(\tau) = 2|r|^4P_0^2R^2\eta^2r_m(\tau)+2\sigma_\kappa^2|r|^2|P_0P_{\text{in}}R^2\eta^2\times \\ &\int_0^L \mathrm{d}z\exp\left(-2\alpha z\right)T_P(z)R_{\text{fiber}}(z,\tau)R_{S_{\Delta\psi}(\omega)}(z,\tau)\left[1+2r_m(\tau)+2r_m(2nz/c)\right]+ \\ &2\sigma_\kappa^2|r|^2P_0P_{\text{in}}R^2\eta^2\int_0^L \mathrm{d}z\exp\left(-2\alpha z\right)\left[r_m(2nz/c+\tau)+r_m(2nz/c-\tau)\right]+O\left(\sigma_\kappa^4\right),\end{aligned} \tag{25}$$

where we have dropped $O(r_m^2)$ terms, and P_{in} denotes the optical power at the entrance of the fiber. The first term in (25) results in from the laser amplitude noise, the second term results in from the beating between the laser and Rayleigh backscattered wave, and the last term from the beating between the laser and Rayleigh intensities. The result of Eq. (25) does not depend on the phase offset γ_0.

For a balanced photo-detector, as depicted in Fig. 1, the intensity noise of the laser source and the Rayleigh backscattering will be partially canceled [38], and the significant term will correspond to the beating between the laser and the Rayleigh backscattered noise. Therefore, Eq. (13) will take the form

$$r_{\text{BPD}}(\tau)/b^2 \approx 2|r|^2|q|^2l^2\,\text{Re}\left\langle \mathbf{E}_R^\dagger(t)\,\mathbf{p}_{\text{ref}}E_s(t)\,E_s{}^*(t-\tau)\,\mathbf{p}_{\text{ref}}^\dagger\mathbf{E}_R(t-\tau)\right\rangle, \tag{26}$$

and we then obtain

$$\begin{aligned}&r_{\text{BPD}}(\tau) \approx 2\sigma_\kappa^2|r|^2|P_0P_{\text{in}}R^2\eta^2\times \\ &\int_0^L \mathrm{d}z\exp\left(-2\alpha z\right)T_P(z)R_{\text{fiber}}(z,\tau)R_{S_{\Delta\psi}(\omega)}(z,\tau)\left[1+2r_m(\tau)+2r_m(2nz/c)\right].\end{aligned} \tag{27}$$

In a typical laser, the angular-frequency noise spectrum $S_{\Delta\psi}(\omega)$ is composed of white noise with a spectral density S_0 and flicker noise with a spectral density $k/|\omega|$ [37, 39, 40] :

$$S_{\Delta\psi}(\omega) = S_0 + \frac{k}{|\omega|}. \tag{28}$$

Substitution of Eq. (28) into Eq. (23) yields

$$R_{S_{\Delta\psi}(\omega)}(z,\tau) = \quad R_{S_0}(z,\tau)R_{k/|\omega|}(z,\tau), \tag{29}$$

where

$$\begin{aligned}R_{S_0}(z,\tau) &= \exp\left[-\frac{4}{\pi}\int_{-\infty}^{\infty}\mathrm{d}\omega\sin^2\left(\frac{\omega\tau}{2}\right)\sin^2\left(\frac{\omega\tau_z}{2}\right)\frac{S_0}{\omega^2}\right], \\ R_{k/|\omega|}(z,\tau) &= \exp\left[-\frac{4}{\pi}\int_{-\infty}^{\infty}\mathrm{d}\omega\sin^2\left(\frac{\omega\tau}{2}\right)\sin^2\left(\frac{\omega\tau_z}{2}\right)\frac{k}{|\omega|^3}\right].\end{aligned} \tag{30}$$

#242975 Received 22 Jun 2015; revised 3 Sep 2015; accepted 4 Sep 2015; published 22 Sep 2015

Performing the integrations in Eq. (30), we obtain the autocorrelation function for the laser white and flicker frequency noise [41]:

$$R_{S_0}(z,\tau)=\begin{cases}\exp(-S_0|\tau|) & |\tau|\le\tau_z\\ \exp(-S_0\tau_z) & |\tau|>\tau_z,\end{cases} \tag{31}$$

$$R_{k/|\omega|}(z,\tau)=\begin{cases}\exp\left[-\frac{1}{2\pi}\tau^2\tau_z^2 k\nu(\tau_z,|\tau|)\right] & |\tau|<\tau_z\\ \exp\left[-\frac{1}{2\pi}\tau^2\tau_z^2 k\nu(|\tau|,\tau_z)\right] & |\tau|>\tau_z\\ \exp\left[-\frac{1}{2\pi}k\tau^2\log 16\right] & |\tau|=\tau_z\\ 1 & \tau=0,\end{cases} \tag{32}$$

where

$$\nu(\chi,\chi_0)=\frac{4\tanh^{-1}(\chi_0/\chi)}{\chi\chi_0}+\frac{2\tanh^{-1}\left(1-2\chi_0^2/\chi^2\right)}{\chi^2}+\frac{\log\left(1-\chi_0^2/\chi^2\right)}{\chi_0^2},\ \chi_0\le\chi. \tag{33}$$

2.1. Computational results

We have calculated the noise spectrum that is induced by the backward Rayleigh scattering by solving Eq. (27). The integration in Eq. (27) was performed with a fiber length resolution of 100 m and a time resolution of 0.1 μs. We have verified that increasing the time and length resolution did not significantly affect the results. We assumed that a balanced photo-detector is used, and we therefore neglected the laser intensity noise that is directly added to the detected spectrum.

Equations (25) and (27) contain a function $T_P(z)$ that varies along the fiber due to random birefringence in fibers. In this paper, we study the noise spectrum that is caused by a laser with a long coherence length, so that the function $R_{S_{\Delta\psi}(\omega)}(z,\tau)$ in Eqs. (25) and (27) does not change significantly on a short length scale that corresponds to the polarization beat length L_B and the polarization correlation length L_C of the fiber, as defined in [34]. This short length scale is on the order of tens of meters [46] while the coherence length of the laser is on the order of kilometers. Therefore, $T_P(z)$ can be approximated in Eqs. (25) and (27) by its spatially-averaged value T_{P_0}, as shown in Appendix A. We find that T_{P_0} varies between $1/3$ to $2/3$, depending on the polarization of the source and on the details of the experimental configuration. We note however that if the measurement time is short compared to the time on which the relative phases between the Rayleigh back-reflections change due to environmental effects, then we expect T_{P_0} to vary between 0 and 1. In the remainder of this paper, we set $T_P(z)=2/3$ in Eqs. (25) and (27).

Figure 2 shows the calculated power spectral density from Eq. (27) (black curve) and the result without adding the flicker noise of the laser (red curve) for a 2-km long optical fiber with parameters that correspond to Corning SMF-28 fiber. We use a fiber loss coefficient $\alpha=0.19$ dB/km and a Rayleigh backscatter coefficient at 1550 nm wavelength for a $T=1$ ns pulse width that is equal to -82 dB [42]. Using Eq. (6) and assumption 3, the optical power that is reflected from a fiber section with a length cT/n equals $P_B=P_{\text{in}}\sigma_\kappa^2 cT/(2n)$. Hence, the variance of the local reflection coefficient κ is given by $\sigma_\kappa^2=2n(P_B/P_{\text{in}})/(cT)=6.1\times10^{-8}$ m^{-1}, where $n=1.45$ is the refractive index of the fiber.

The laser had a white angular-frequency noise parameter $S_0=3.9478\times10^3$ $(\text{rad/s})^2/\text{Hz}$ and a flicker angular-frequency noise parameter $k=1.3643\times10^8$ $(\text{rad/s})^3/\text{Hz}$. The corresponding laser linewidth for a 1-ms measurement duration approximately equals 3 kHz [43]. The coupling fractions are $|r|^2=0.25$, $|q|^2=0.75$. The other parameters are the optical power

#242975 Received 22 Jun 2015; revised 3 Sep 2015; accepted 4 Sep 2015; published 22 Sep 2015

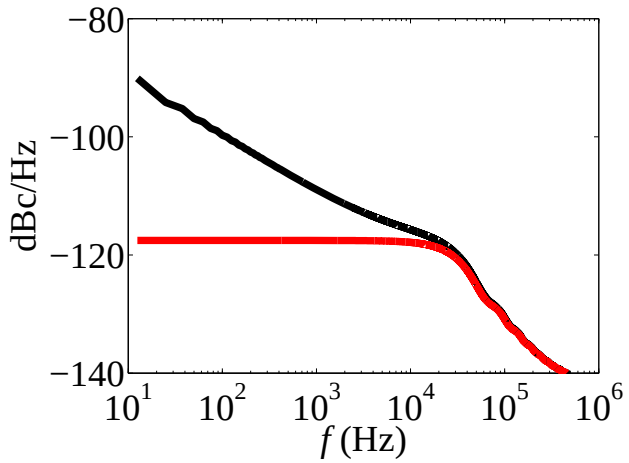

Fig. 2. Power spectral density of the detected backward Rayleigh wave that is calculated by numerically solving Eq. (27) (black curve) for a 2-km fiber in a self-homodyne detection system. The polarization factor $T_P(z)$ was approximated by its spatially averaged value $2/3$. The figure also shows the spectrum in case that the laser flicker noise is set to zero (red curve). The coherence length of the laser, as defined by a laser white frequency noise source (76 km) is longer than the fiber length (2 km). The laser linewidth for a 1 ms observation time is approximately 3 kHz. The fiber parameters correspond to Corning SMF-28 fiber.

at the entrance of the fiber is $P_{\text{in}} = 0$ dBm, the photo-detector efficiency is $\eta = 1$ A/W, and the electrical resistance is $R = 50\ \Omega$. These parameters correspond to the laser and fiber parameters that were used in our experiment, as described in section 3. An additional high-frequency phase noise that is unique to the laser used in our experiments, was not added to the results given in this section. This noise source was added in section 3 in which we compare the theoretical and experimental results.

The parameters of the phase noise induced by the fiber (see "Table II" in [20]) are α_1 equals to 1.9×10^{-16} rad^2/Hz/m and α_2 equals to 2×10^{-12} rad^2/m.

The power spectral density of the detected signal was normalized by the RF power at the photo-detector: $|r|^2|P_0P_{\text{in}}R^2\eta^2$. The relative intensity noise of the laser was modeled by an empirical fit to the measured noise: $\text{RIN}(f) = -100 - 12\log_{10}(f)$ (dBc/Hz).

The spectrum shown in Fig. 2 can be divided into two frequency regions. At high frequencies for which $f > c/(2Ln)$, the spectrum is determined by the laser white frequency noise and the slope of the spectrum equals $1/f^2$. At frequencies between about 200 Hz to $c/(2Ln)$ the spectrum is affected by the laser flicker frequency noise and its slope equals about $1/f$. We will show that, as the fiber length increases, the laser flicker frequency noise becomes the dominant effect at low frequencies, and it has a complex dependence on the fiber length.

In the numerical calculations, we did not observe a significant effect of the fiber phase noise due to the thermal and mechanical fluctuations on the noise spectrum. In [20], the phase noise was measured in an interferometric system where the difference between the interferometer arms length was a few centimeters and hence the effect of the laser frequency noise is very small. In our system, the length difference between the two interferometer arms can be on the order of kilometers and hence the dominant noise is the laser frequency noise, so that in our experiments $R_{\text{fiber}}(z,\tau) \approx 1$.

#242975 Received 22 Jun 2015; revised 3 Sep 2015; accepted 4 Sep 2015; published 22 Sep 2015

3. Comparison with the experiment results

We have validated the model by comparing its results to measurements conducted in experiments that are described in [9]. The experiment setup is shown in Fig. 1. The source in the experiments was a long coherence laser—"Teraxion-NLL" with a specified linewidth smaller than 5 kHz [44]. The corresponding coherence length, as defined only by the laser white frequency noise was about 76 km [45]. However, the laser linewidth is broadened by the laser flicker frequency noise and it approximately equals 3 kHz for a 1 ms measurement duration [43].

In the experiments the fiber length was varied between 500 m to 173.4 km and the variable optical attenuator was adjusted to provide an input power of 0 dBm. The coupling coefficients $|r|^2$ and $|q|^2$ were 0.25 and 0.75 respectively and the spectrum was measured by using an electronic cross-spectrum analyzer.

In addition to a white and flicker frequency noise, our experiments had additional high-frequency noise [44]. We add this noise to our model in order to obtain a good comparison between theory and experiments at frequencies above 100 kHz.

The laser angular-frequency noise was modeled by

$$S_{\Delta\psi}(\omega) = S_0 + \frac{k}{|\omega|} + S_{\mathrm{HF}}(\omega), \tag{34}$$

where

$$S_{\mathrm{HF}}(\omega) = a|\omega|^3, \ |\omega| \le \omega_1. \tag{35}$$

The parameters were chosen to obtain the best fit between theory and a direct measurement of the source [44]: $S_0 = 3.9478 \times 10^3 \ (\mathrm{rad/s})^2/\mathrm{Hz}$, $k = 1.3643 \times 10^8 \ (\mathrm{rad/s})^3/\mathrm{Hz}$, $a = 7.9577 \times 10^{-15} \ (\mathrm{rad/s})^{-1}/\mathrm{Hz}$, and $\omega_1 = 2\pi \times 2$ MHz.

To include the additional high frequency noise contribution, Eq. (30) is modified to

$$R_{S_{\Delta\psi}(\omega)}(z,\tau) = R_{S_0}(z,\tau) R_{k/|\omega|}(z,\tau) R_{\mathrm{HF}}(z,\tau), \tag{36}$$

where $R_{\mathrm{HF}}(z,\tau)$ is calculated from Eq. (34) using Eq. (23).

Figure 3 shows the self-homodyne-detected backward Rayleigh spectrum, measured for several fiber lengths (solid blue curves). The experimental data is compared to the theoretical results (dashed green curves), calculated using Eq. (27) with $T_P(z) = 2/3$. Good agreement between theory and experimental data is obtained at frequencies above 200 Hz for fiber lengths between 6 to 100 km. For shorter fibers with a length between 500 m to 6 km, a good agreement was obtained only at frequencies that are higher than 500 Hz. The measurements indicate the existence of a low-frequency noise source that is not included in our model. This noise source becomes more important as the fiber length decreases. By analyzing the experimental results at very low frequencies of about 10 Hz, we find that the power density of this noise source grows linearly by about 4 dB per kilometer when the fiber length is changed between 500 m to 3 km. For longer fibers ($6-100$ km), the power of this noise source is approximately constant. Also, the spectral shape of this low frequency noise does not change significantly as a function of the fiber length. This noise might be due to the receiver, due to excess low-frequency intensity noise of the specific laser used in the experiment, or due to environmental noise. For fibers longer than about 6 km, the noise induced by the laser flicker frequency noise becomes the dominant noise source at frequencies as low as 200 Hz.

We have also compared the theoretical and experimental dependence of the power spectral density on the fiber length at two specific frequencies as shown in Fig. 4. A very good quantitative agreement is obtained for fiber lengths between 500 m to 20 km. We find that the noise at a frequency around 1 kHz, where the laser flicker noise is the dominant noise source, grows

#242975 Received 22 Jun 2015; revised 3 Sep 2015; accepted 4 Sep 2015; published 22 Sep 2015

as a function of the fiber length as $L^{2.4\pm0.1}$. The power dependence on the fiber length varies as a function of the laser frequency flicker noise amplitude.

At higher frequency $f = c/(2nL)$, where the laser white frequency noise is the dominant noise source, the noise spectrum grows as a function of the fiber length as $L^{3\pm0.2}$. This result is verified analytically using a simplified model that is given in the Appendix B.

#242975 Received 22 Jun 2015; revised 3 Sep 2015; accepted 4 Sep 2015; published 22 Sep 2015

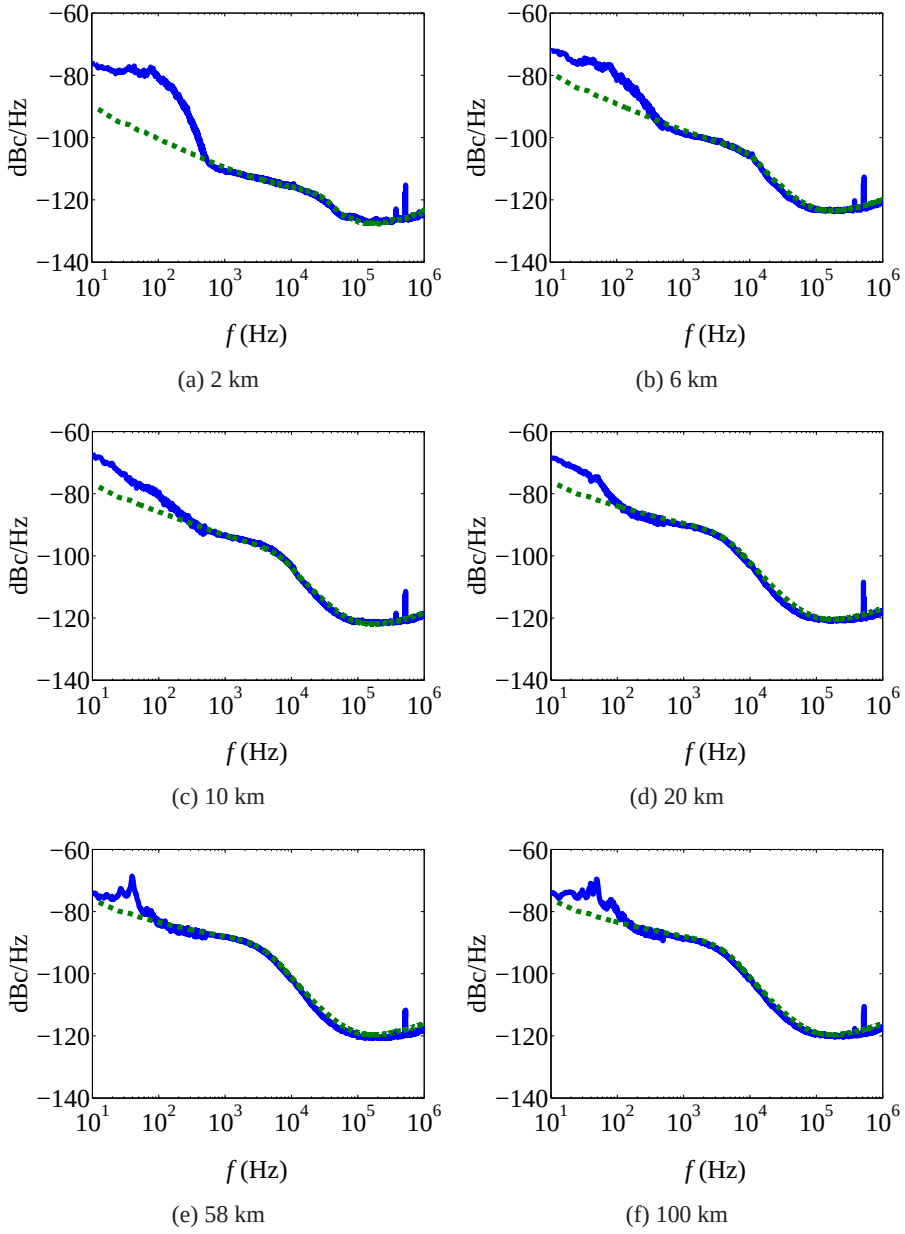

(a) 2 km (b) 6 km

(c) 10 km (d) 20 km

(e) 58 km (f) 100 km

Fig. 3. Comparison between theory (dashed green curves) and experiment (solid blue curves) for the noise power spectral density for various fiber lengths: (a) 2 km, (b) 6 km, (c) 10 km, (d) 20 km, (e) 58 km and (f) 100 km. The input optical power was 0 dBm. The parameters of the fiber and coupling fractions that were used in the numerical calculations are the same as given in section 2.1. A balanced photo-detector was used. The coherence length of the laser that was used in the calculations is 76 km, assuming white frequency laser noise and a total linewidth of 3 kHz for a 1-ms observation time. Good agreement between theory and experiments is obtained for fiber lengths greater than 6 km and all the fiber lengths at frequencies above 200 Hz.

#242975 Received 22 Jun 2015; revised 3 Sep 2015; accepted 4 Sep 2015; published 22 Sep 2015

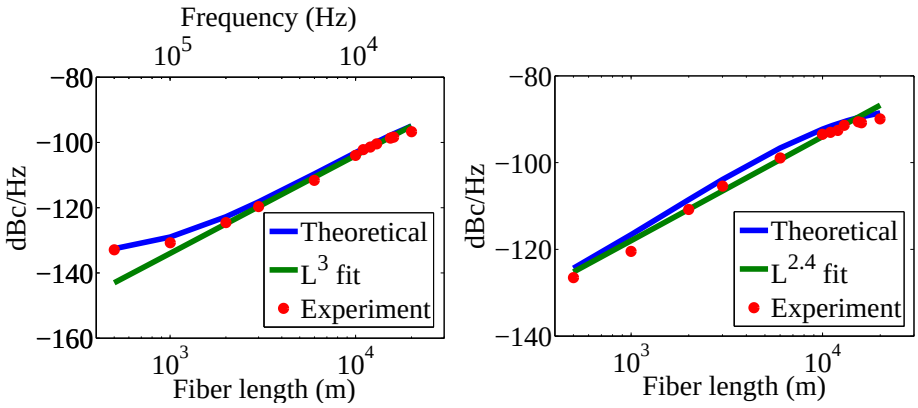

(a) $f = c/(2nL)$ (b) $f = 1$ kHz

Fig. 4. Power spectral density of the detected noise vs. fiber length (L). We compare theoretical results (blue curves), experimental results (red dots), and empirical fits (green curves). In (a), we allow the frequency to vary, so that $f = c/(2nL)$. At $L = 5$ km, the frequency is 21 kHz, at $L = 20$ km, the frequency is 5 kHz. The power spectral density is approximately proportional to L^3. In (b), we set $f = 1$ kHz. The power spectral density is approximately proportional to $L^{2.4}$.

4. Conclusions

We describe a comprehensive theoretical model for studying intensity noise induced in optical fibers by spontaneous Rayleigh backscattering that is detected by a self-homodyne scheme. The model includes laser frequency noise, laser amplitude noise, random distribution of Rayleigh scatterers along the fiber, phase noise that is induced in the optical fibers due to thermal and mechanical fluctuations, and fiber loss. The results indicate that the dominant noise source at frequencies of about 500 Hz is the laser flicker frequency noise. At higher frequencies of about 10 kHz, the noise is dominated by the white frequency noise of the laser. We compared the calculated self-homodyne detected noise spectrum to experimental results for a laser with a linewidth of about 3 kHz. Although the noise spectrum due to Rayleigh backscattering has a complex dependence on the fiber length, a good agreement between theory and experiment is obtained for fiber lengths between 6 to 100 km at frequencies above 200 Hz. For shorter fibers with lengths between 500 m to 6 km, good agreement was obtained only at higher frequencies of more than about 500 Hz.

5. Appendix A–calculation of the average polarization coefficient T_{P_0} for a long coherence length laser

Equations (25) and (27) contain a function $T_P(z)$ that changes randomly due to the optical fiber's birefringence that varies randomly as a function of position. However, the fiber birefringence changes on a time scale that is larger than a few minutes even for long fibers with a length on the order of tens of kilometers [21]. The polarization change of waves and in particular backscattered waves in fibers with a random birefringence was modeled in [25, 26, 34]. In the case of a polarization maintaining fiber, the polarization of the reflected wave will be equal to the polarization of the incident wave as long as the input wave is linearly polarized along one of the principal axes of the fiber, and therefore $T_P(z) = 1$ for all z.

The integral in Eqs. (25) and (27) contains functions that change on different length scales.

#242975 Received 22 Jun 2015; revised 3 Sep 2015; accepted 4 Sep 2015; published 22 Sep 2015

The short length scale, on the order of tens of meters, corresponds to the fiber beat length and the fiber correlation length [46]. On the other hand, the laser coherence length for the laser used in the experiments and the fiber attenuation length $1/\alpha$ are on the order of kilometers. Hence, the function $T_P(z)$ varies on a short length scale, while other functions in the integral vary on a long length scale. Assuming that the fiber length is significantly longer than the short length scale, the rapidly varying function $T_P(z)$ can be replaced in calculating the integral by its spatial average. This result can be obtained by using the first mean value theorem (see [41], p. 1063). We calculate the integral by dividing the integration interval into sections, each with a length d, that is significantly longer than the short length scale and is shorter than the long length scale. Assuming that the section length d is sufficiently long, the function $T_P(z)$ can be approximately replaced in each section by its spatial average while the variation of the other functions in the section can be neglected. Therefore, the random process $T_P(z)$ in Eqs. (25) and (27) can be approximately replaced by its spatial average T_{P_0} that is calculated using Eq. (19), so that

$$T_{P_0} = \frac{1}{2}\left[1 + \mathbf{s}_{\text{ref}} \cdot \langle \mathbf{s}(z) \rangle_z\right], \tag{37}$$

where $\mathbf{s}_{\text{ref}}$ is the state of polarization (SOP) of the source wave at the photo-detector and

$$\langle \mathbf{s}(z) \rangle_z = \frac{1}{d} \int_z^{z+d} \mathrm{d}z' \mathbf{s}(z') \tag{38}$$

denotes a spatial average of the Stokes vector of the backscattered wave at any section along the fiber.

To calculate T_{P_0}, we need to determine the spatial average $\langle \mathbf{s}(z) \rangle_z$ of the backscattered wave at the photo-detector. In [25], the time average of the DOP of the backscattered wave was calculated for a laser with a coherence length that is significantly shorter than the fiber length. It was assumed that different reflections along the fiber are incoherently added so that the corresponding Mueller matrices of their reflections can be added as well. The average polarization of the backscattered wave was determined by the expectation value of the Mueller matrix. It was shown that the backscattered SOP is identical to the input SOP and the DOP reduces to $1/3$ of the source DOP. It was also shown experimentally that the fluctuation of the backscattered wave decreases as the coherence length of the laser is decreased. In the experiments that are described in Sec. 3, the coherence length of the laser is longer than the fiber length. Nonetheless, the same result will hold as long as the measurement time is long compared to the time scale for environmental changes. In this case, we find $T_{P_0} = (1/2)\left[1 + \mathbf{s}_{\text{ref}} \cdot \mathsf{M}_2\mathsf{M}_1\mathbf{s}_0/3\right]$, which varies between $1/3$ and $2/3$, depending on the states of polarization of the reference and the reflected waves at the photo-detector. In the other limit where the detection time is short, we expect T_{P_0} to vary between 0 and 1.

In the calculated results given in this paper we set $T_P(z) = T_{P_0} = 2/3$.

6. Appendix B – Simplified model for a laser with only a white frequency noise

It is possible to obtain a closed-form analytical expression for the self-homodyne detected noise spectrum of the Rayleigh backscattered noise. This approximation is accurate for high frequency noise [$f > c/(2nL)$]. The analytical model is valid for a laser with an arbitrary coherence length. In the special case that the laser coherence length is significantly shorter than the fiber length, the spectrum approaches a Lorentzian shape as obtained in [6].

We observe in Fig. 2 that at high frequencies [$f > c/(2nL)$] the main noise source contributing to the Rayleigh backscattered noise is the white frequency noise of the laser. Therefore, to obtain insight into the properties of the backscattered Rayleigh noise spectrum at frequencies

#242975 Received 22 Jun 2015; revised 3 Sep 2015; accepted 4 Sep 2015; published 22 Sep 2015

greater than $c/(2nL)$, we present a simplified model in which it is assumed that the laser flicker and amplitude noise can be neglected. In this case, Eq. (27)–(39) can be solved analytically to obtain a solution even when that the coherence length of the laser is longer than the fiber length.

The one-sided spectrum of the Rayleigh backscattered noise is defined as

$$S(\omega) = 2\int_{-\infty}^{\infty} \mathrm{d}\tau\, r(\tau)\exp\left(-j\omega\tau\right), \tag{39}$$

where $r(\tau)$ is given by Eq. (25).

By ignoring the fiber losses ($\alpha = 0$), fiber phase fluctuations [$R_{\mathrm{fiber}}(z,\tau) = 1$], laser amplitude and flicker frequency noise, Eq. (39) simplifies to

$$\begin{aligned} S(\omega)/u = {} & T_{P_0}\frac{\pi c\delta(\omega)\left[1-\exp\left(-2LnS_0/c\right)\right]}{nS_0} + \\ & T_{P_0}\frac{S_0}{n\omega\left(S_0^2+\omega^2\right)^2}\times\left[2\omega\left(Ln\left(S_0^2+\omega^2\right)-cS_0\right)+\exp\left(-\frac{2LnS_0}{c}\right)c\left(S_0^2-\omega^2\right)\sin\left(\frac{2Ln\omega}{c}\right)\right] + \\ & T_{P_0}\frac{2S_0^2}{n\left(S_0^2+\omega^2\right)^2}\times\exp\left(-\frac{2LnS_0}{c}\right)c\cos\left(\frac{2Ln\omega}{c}\right), \end{aligned} \tag{40}$$

where $u = 4\sigma_\kappa^2|r|^2P_0P_{\mathrm{in}}R^2\eta^2$. A useful result is obtained by evaluating Eq. (40) at the frequency $\omega_L = 2\pi c/(2Ln)$ in the limit that the coherence length of the laser is greater than the fiber length, i.e., $2LnS_0/c \ll 1$, so that

$$S\left(\omega_L\right)/u \approx T_{P_0}\frac{2L^3n^2S_0}{c^2\pi^2} \tag{41}$$

and

$$S(\omega\to 0)/S(\omega_L) \approx 2\pi^2/3. \tag{42}$$

In this limit, we find that ω_L equals the noise bandwidth of the Rayleigh backscattered spectrum when the coherence length of the laser is greater than the fiber length. The noise amplitude at this frequency is proportional to L^3. This dependence occurs for a laser with a coherence length that is longer than the fiber since a reflection from a location z that interferes with the laser source adds a noise power that is proportional to z^2. Incoherent integration of the independent reflections along the fiber gives another factor of length resulting in a dependency of the noise power that is proportional to L^3. In another case when the fiber length is much longer than the coherence length of the laser, Eq. (40) approaches a Lorentzian shape,

$$S\left(\omega\right)/u \approx T_{P_0}\frac{2S_0L}{S_0^2+\omega^2}. \tag{43}$$

This result was obtained in [6]. In this case, the noise bandwidth does not depend on the fiber length, and the noise amplitude is proportional to L.

Acknowledgments

Work at the Technion was supported by the Israel Science Foundation (ISF) of the Israeli Academy of Sciences (grant No. 1092/10). Work at the UMBC was supported by the Army Research Laboratory.